Chemistry & Biology, Volume *22*

Supplemental Information

Differential Regulation of Specific Sphingolipids in Colon Cancer Cells during Staurosporine-Induced Apoptosis

Virginia del Solar, Darleny Y. Lizardo, Nasi Li, Jerod J. Hurst, Christopher J. Brais, and G. Ekin Atilla-Gokcumen

Supplemental Data

Figure S1. **Viability assay for colon cell lines and PARP cleavage in non-cancerous and cancerous cell lines** (related to Figure 1A, Figure 5C and Supplemental Experimental Procedure "Cell culture and treatments").

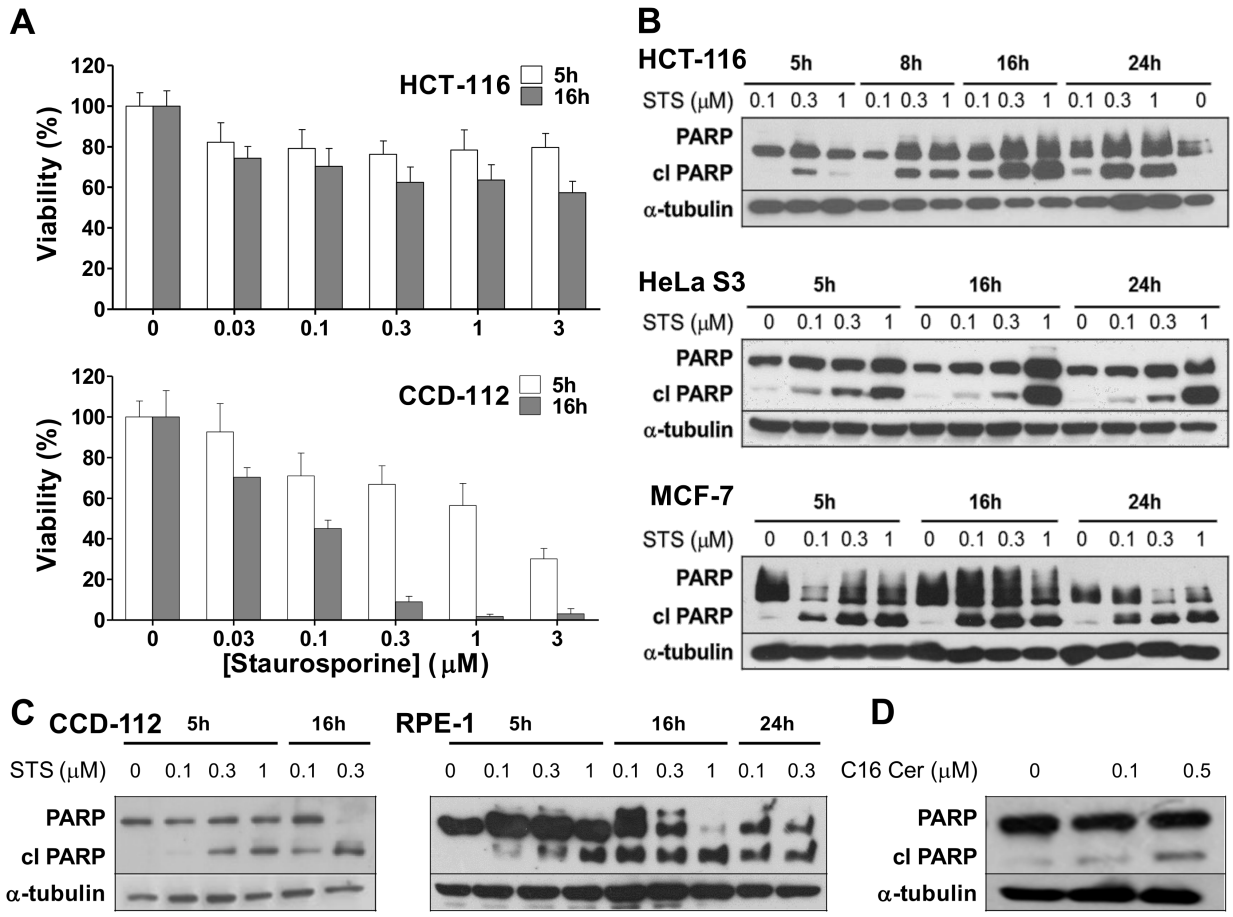

(A) Cell viability in the presence of different concentrations of staurosporine in HCT-116 and CCD-112 colon cells. Data from three independent experiments (n = 15) are shown as mean ± SD. (B-C) Western blots of cell lines treated for 5-24 hours with DMSO (0) and staurosporine (STS) at different concentrations. Lysates were analyzed for PARP and α-tubulin. Two bands are shown in PARP, full-length PARP (116 kDa) and cleaved (cl) PARP (89 kDa). The cleaved form is a marker of apoptosis; α-tubulin was used as loading control. (B) Cancer cell lines: HCT-116, human colorectal carcinoma; HeLa S3, human cervical carcinoma; MCF-7, human breast adenocarcinoma. (C) Non-cancer cell lines: CCD-112, human colon fibroblast; RPE-1, human retinal pigmented epithelium. (D) Western Blot of HCT-116 cell line treated with C16-ceramide (C16 Cer) at different concentrations during 16h.

Figure S2. PARP cleavage and ceramide/dihydroceramide fold changes in HCT-116 cells after doxorubicin treatment (related to Table 1).

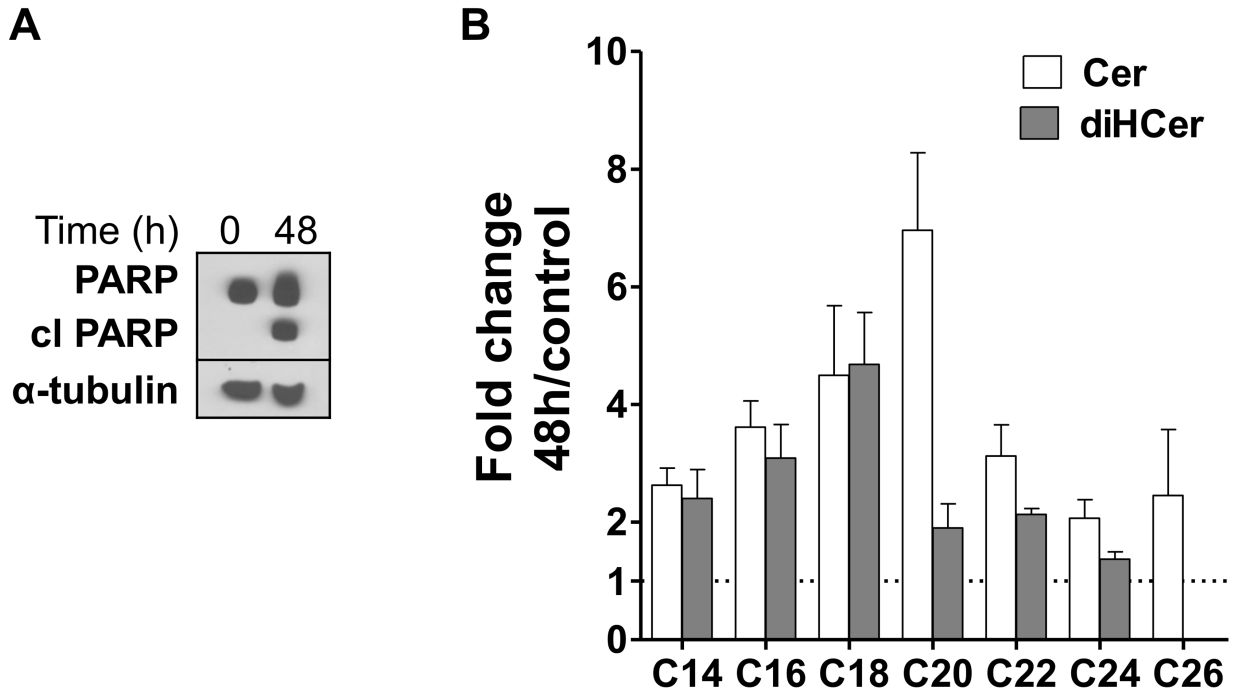

(A) Western blot of HCT-116 treated with DMSO (0) or 2 μM doxorubicin for 48 h. Lysates were analyzed for PARP and α-tubulin. Two bands are shown in PARP, full-length PARP (116 kDa) and cleaved (cl) PARP (89 kDa). The cleaved form is a marker of apoptosis; α-tubulin was used as loading control. (B) Fold changes in ceramide and dihydroceramide levels in HCT-116 cells after 2 μM doxorubicin treatment for 48h. Dotted line indicates no change (Fold change=1). Data from two independent experiments (n = 10) are shown as mean ± SD. For each ceramide and dihydroceramide fold difference is determined as [$Abundance_{48h\text{-}treatment}$] / [$Abundance_{control}$]. Abundance is the total ion count for a given ion. Lipid composition was normalized based on protein concentration and internal standards. Dotted line indicates equal levels in both treated and non-treated cells.

Figure S3. **Effect of staurosporine and C16-ceramide combination treatment on viability of HCT-116 cells** (related to Figure 5C).

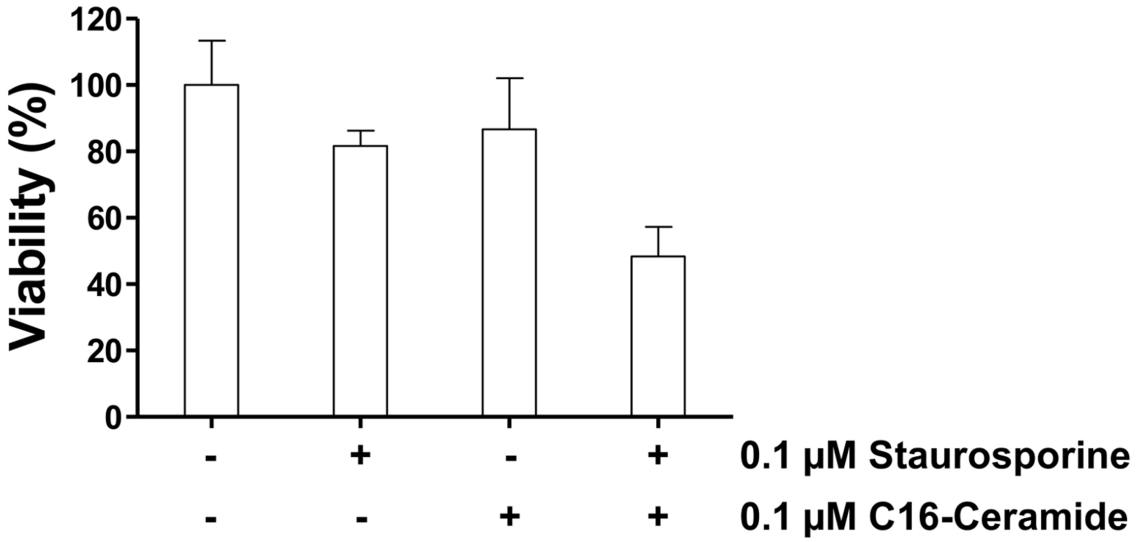

MTT assay was performed to determine the viability of HCT-116 cell line treated with either staurosporine (0.1 µM) or C16-ceramide (0.1 µM) or in combination of both compounds for 16 hours. Data from two independent experiments (n = 10) are shown as mean ± SD.

Table S1. Matrix effect and quantification of ceramides in HCT-116 and CCD-112 cells. $^{13}C_{18}$-Oleic acid and C17-Ceramide were used as internal standards in matrix effect evaluation[a] (related to Figure 5A and Experimental Procedure "Preparation of Lipid Extracts, LC-MS Method and Data Analysis" and Supplemental Experimental Procedure "Normalization and the matrix effect" and "Quantification of ceramides by LC-MS").

Area	**CCD-112**	**HCT-116**	[ng/mg]	**CCD-112**	**HCT-116**	**Ratio[f]**
$^{13}C_{18}$-Oleic acid[b] *m/z* = 299.3090[e]	6.52 ± 0.56E+06	6.20 ± 1.24E+06	**C14 Cer**	1.34 ± 0.01	1.44 ± 0.17	0.93
C17 Cer[c] *m/z* = 550.5205[e]	1.31 ± 0.11E+07	1.55 ± 0.17E+07	**C16 Cer**	3.38 ± 0.38	4.05 ± 0.81	0.83
C14:0 FA[d] *m/z* = 227.2017[e]	1.33 ± 0.05E+07	1.43 ± 0.18E+07	**C22 Cer**	0.30 ± 0.02	0.18 ± 0.03	1.67
C16:0 FA[d] *m/z* = 255.2330[e]	6.85 ± 1.86E+07	5.73 ± 0.94E+07	**C24 Cer**	4.25 ± 0.35	2.02 ± 0.14	2.10

[a] Data are given as average ± SD of three independent experiments. [b] Area was determined as (Abundance) / [$^{13}C_{18}$-Oleic acid]. Abundance is the total ion count for a given ion. Each ion corresponds to a mass-to-charge ratio (*m/z*), which is used to assign the specie. [c] Area was determined as (Abundance) / [C17 Cer]. [d] FA, fatty acid. Area was determined as (Abundance) of specific lipid *m/z*. [e] *m/z*'s corresponding to $[M-H]^-$. No significant differences in abundances were observed due to matrix effect between HCT-116 and CCD-112 ($p \geq 0.1$). [f] Ratio was determined as $[\text{ng/mg protein}]_{\text{CCD-112}}$ / $[\text{ng/mg protein}]_{\text{HCT-116}}$ for each ceramide.

Table S2. Targeted analysis of lipids during apoptosis in HCT-116 cells[a] (related to Figure 2).

Lipid family	Lipid	*m/z*	RT	FC[b] (16h/C)	Lipid	*m/z*	RT	FC (16h/C)	Lipid	*m/z*	RT	FC (16h/C)
FA[c]	**C14:0**	227.2011	31.9	0.9	**C18:1**	281.2481	35.6	1.1	**C24:0**	367.3576	45.3	1.4
	C16:0	255.2324	34.9	1.0	**C18:2**	279.2324	34.0	1.1	**C24:1**	365.3420	42.8	1.5
	C16:1	253.2168	32.8	1.1	**C20:0**	311.2950	40.3	1.0	**C26:0**	395.3889	47.6	1.2
	C18:0	283.2637	37.5	1.1	**C20:4**	303.2324	34.4	0.9				
PA[c]	**LPA C16:0**	409.2355	47.6	0.7	**C34:1**	673.4808	41.6	0.5	**C36:2**	699.4965	42.2	1.1
	C32:0	647.4652	39.7	0.3	**C34:2**	671.4652	40.3	0.6	**C36:3**	701.5121	43.7	1.1
	C32:1	645.4495	41.0	0.4	**C36:1**	697.4808	41.1	0.8	**C38:4**	723.4965	43.0	1.5
PE[c]	**LPE C18:0**	480.3090	39.9	0.5	**LPE C20:4**	500.2777	36.1	0.6	**C36:2**	742.5387	52.9	0.8
	LPE C18:1	478.2934	37.7	0.7	**C36:1**	744.5543	54.5	0.6	**C38:4**	766.5387	53.6	0.5
PS[c]	**LPS C18:0**	524.2988	32.1	1.0	**C34:1**	760.5129	42.7	1.2	**C36:4**	782.4972	42.7	1.1
	LPS C18:1	522.2832	30.3	1.2	**C34:2**	758.4972	41.3	1.8	**C38:4**	810.5285	44.0	2.5
	C32:0	734.4972	42.0	0.8	**C36:1**	788.5442	44.7	1.1	**C38:5**	808.5129	43.1	1.5
	C32:1	732.4816	40.7	1.3	**C36:2**	786.5285	43.1	1.6				
PI[c]	**LPI C18:0**	599.3196	37.7	1.5	**C34:1**	835.5337	49.2	1.1	**C36:4**	857.5180	48.3	1.1
	LPI C18:1	597.3040	35.6	1.6	**C34:2**	833.5180	47.7	1.4	**C38:4**	885.5493	50.5	1.2
	C32:0	809.5180	48.7	0.7	**C36:1**	863.5650	51.2	1.5	**C38:5**	883.5337	48.8	1.3
	C32:1	807.5024	47.3	1.1	**C36:2**	861.5493	49.7	1.3				
ST[d]	**Cholesterol**	369.3521	67.0	1.0								
PC[e]	**LPC C16:0**	496.3403	44.6	1.0	**C34:1**	760.5856	57.9	0.9	**C36:3**	784.5856	57.6	0.9
	LPC C18:0	524.3716	47.3	1.1	**C34:2**	758.5700	57.1	1.0	**C36:4**	782.5700	57.3	0.9
	LPC C18:1	522.3560	45.5	1.3	**C34:3**	756.5543	56.2	1.1	**C38:4**	810.6013	58.7	1.0
	C32:0	734.5700	57.3	0.7	**C36:1**	788.6169	59.2	1.0	**C38:5**	808.5856	57.6	0.8
	C32:1	732.5543	56.6	0.9	**C36:2**	786.6013	58.3	0.9				
DG[d,e]	**C32:0**	551.5039	57.9	0.3	**C36:1**	605.5509	59.6	0.9	**C38:4**	627.5352	59.0	1.2
	C32:1	549.4883	56.2	0.6	**C36:2**	603.5352	58.7	0.9	**C38:5**	643.5302	61.0	0.6
	C34:1	577.5196	58.4	0.6	**C36:3**	601.5196	57.2	2.1				
	C34:2	575.5039	57.6	1.1	**C36:4**	599.5039	56.9	1.1				
TG[f]	**C50:1**	850.7864	66.6	0.7	**C54:3**	902.8177	66.9	2.3	**C56:2**	932.8646	67.6	0.8
	C52:2	876.8020	66.8	1.4	**C54:4**	900.8020	66.6	2.3	**C56:6**	924.8020	66.5	2.3
	C54:2	904.8330	67.2	1.3	**C54:6**	896.7707	66.1	2.0	**C56:8**	920.7707	66.1	2.7

[a] Abbreviations: RT, retention time; FC, fold change; 16h, 16h staurosporine-treated cells; C, control cells; FA, fatty acid; PA, phosphatidic acid; PE, phosphatidylethanolamine; PS, phosphatidylserine; PI, phosphatidylinositol; ST, sterol; PC, phosphatidylcholine; DG, diacylglycerol; TG, triacylglycerol. [b] FC was determined as [Abundance 16h] / [Abundance C] for each lipid. Abundance is the total ion count for a given ion. Each ion corresponds to a mass-to-charge ratio (*m/z*), which is used to assign the lipid species. [c] *m/z*'s corresponding to $[M-H]^-$. [d] *m/z*'s corresponding to $[M+H-H_2O]^+$. [e] *m/z*'s corresponding to $[M+H]^+$. [f] *m/z*'s corresponding to $[M+NH_4]^+$.

Table S3. Targeted analysis of ceramides, dihydroceramides, sphingomyelins and dihydrosphingomyelins during apoptosis in non-cancerous (CCD-112) and cancerous (HCT-116) colon cell lines[a-c] (related to Figure 5A and Figure 5B).

CCD-112							HCT-116						
Acyl chain	**Lipid**	**FC[d] (5h/C)**	**FC[d] (16h/C)**	**Lipid**	**FC (5h/C)**	**FC (16h/C)**	**Acyl chain**	**Lipid**	**FC (5h/C)**	**FC (16h/C)**	**Lipid**	**FC (5h/C)**	**FC (16h/C)**
C14	**Cer**	0.8	1.3	**SM**	0.6	1.1	**C14**	**Cer**	1.0	5.4	**SM**	1.2	3.0
	diHCer[e]	-	-	**diHSM**	1.1	1.6		**diHCer**	6.2	12.4	**diHSM**	2.5	6.1
C16	**Cer**	0.6	1.3	**SM**	0.8	1.1	**C16**	**Cer**	0.5	5.0	**SM**	1.1	1.5
	diHCer	2.4	4.0	**diHSM**	1.6	2.2		**diHCer**	3.0	11.9	**diHSM**	2.4	4.4
C18	**Cer**	0.9	1.2	**SM**	1.0	1.1	**C18**	**Cer**	0.9	5.0	**SM**	1.5	2.4
	diHCer[e]	-	-	**diHSM[e]**	-	-		**diHCer**	5.8	13.8	**diHSM[e]**	-	-
C20	**Cer[e]**	-	-	**SM[e]**	-	-	**C20**	**Cer**	0.9	4.6	**SM[e]**	-	-
	diHCer[e]	-	-	**diHSM[e]**	-	-		**diHCer**	4.2	8.5	**diHSM[e]**	-	-
C22	**Cer**	0.6	1.0	**SM**	0.9	1.2	**C22**	**Cer**	5.2	13.8	**SM**	1.5	3.3
	diHCer	1.8	2.8	**diHSM[e]**	-	-		**diHCer**	2.0	3.0	**diHSM[e]**	-	-
C24	**Cer**	0.7	1.0	**SM**	0.9	1.4	**C24**	**Cer**	2.0	5.1	**SM**	1.3	3.5
	diHCer	1.3	2.1	**diHSM[e]**	-	-		**diHCer**	1.2	2.0	**diHSM**	1.3	3.9
C26	**Cer**	1.5	2.2	**SM**	0.7	1.9	**C26**	**Cer**	2.2	3.9	**SM**	1.1	4.7
	diHCer[e]	-	-	**diHSM[e]**	-	-		**diHCer[e]**	-	-	**diHSM[e]**	-	-

[a] Abbreviations: FC, fold change; 5h, 5h staurosporine-treated cells; 16h, 16h staurosporine-treated cells; C, control cells. [b] Ceramides and dihydroceramides: *m/z*'s corresponding to $[M-H]^-$. Sphingomyelins and dihydrosphingomyelins: *m/z*'s corresponding to $[M]^+$. [c] *m/z*'s and the corresponding RT for each species can be found in the Supplemental Lipid Assignments. [d] FC was determined as [Abundance 16h or 5h] / [Abundance C] for each lipid. Abundance is the total ion count for a given ion. Each ion corresponds to a mass-to-charge ratio (*m/z*), which is used to assign the lipid species. [e] Not detected.

Table S4. Targeted analysis of ceramides and dihydroceramides released into the culture media during apoptosis in HCT-116[a,b] (related to Figure 3 and Supplemental Experimental Procedure "Media extraction").

Lipid	Observed *m/z*	RT	FC (16h/C)[c]	Lipid	Observed *m/z*	RT	FC (16h/C)
C14 Cer	508.4818	62.2	Accum[d]	**C14 diHCer**	510.4923	62.8	Accum[d]
C16 Cer	536.5067	64.0	2.6	**C16 diHCer**	538.5215	64.5	2.5
C18 Cer[e]	-	-	-	**C18 diHCer**[e]	-	-	-
C20 Cer[e]	-	-	-	**C20 diHCer**[e]	-	-	-
C22 Cer	620.6046	68.1	1.1	**C22 diHCer**	622.6160	68.5	1.0
C24 Cer	648.6360	69.6	1.2	**C24 diHCer**	650.6509	70.1	1.1
C26 Cer[e]	-	-	-	**C26 diHCer**[e]	-	-	-

[a] Abbreviations: RT, retention time; FC, fold change; 16h, 16h staurosporine-treated cells; C, control cells; Accum, accumulation. [b] *m/z*'s corresponding to $[M-H]^-$. [c] FC was determined as [Abundance 16h] / [Abundance C] for each lipid. Abundance is the total ion count for a given ion. Each ion corresponds to a mass-to-charge ratio (*m/z*), which is used to assign the lipid species. [d] Not detected in control. Fold increase could not be determined due to the low abundance in control cells. [e] Not detected.

Table S5. Targeted analysis of ceramides and dihydroceramides during apoptosis in non-cancerous (RPE-1) and cancerous (HeLa S3 and MCF-7) cells[a-c] (related to Figure 5A).

RPE-1				HeLa S3				MCF-7			
Acyl chain	**Lipid**	**FC[d] (5h/C)**	**FC[d] (16h/C)**	**Acyl chain**	**Lipid**	**FC (5h/C)**	**FC (16h/C)**	**Acyl chain**	**Lipid**	**FC (5h/C)**	**FC (16h/C)**
C14	**Cer**	1.4	2.0	**C14**	**Cer**	1.5	3.0	**C14**	**Cer**	1.9	4.0
	diHCer	1.3	1.4		**diHCer**	3.0	7.4		**diHCer**	5.6	19.5
C16	**Cer**	1.4	1.6	**C16**	**Cer**	1.1	2.4	**C16**	**Cer**	1.4	3.8
	diHCer	2.4	1.6		**diHCer**	2.5	5.3		**diHCer**	3.6	10.1
C18	**Cer**	1.7	1.2	**C18**	**Cer**	0.9	1.6	**C18**	**Cer**	1.5	5.8
	diHCer	1.9	1.2		**diHCer**	1.9	5.7		**diHCer**	5.0	24.8
C20	**Cer**	1.5	1.2	**C20**	**Cer**	1.3	2.6	**C20**	**Cer**	1.8	7.6
	diHCer	1.3	1.1		**diHCer**	1.4	2.8		**diHCer**	5.0	24.7
C22	**Cer**	1.5	1.5	**C22**	**Cer**	1.5	3.1	**C22**	**Cer**	1.3	3.5
	diHCer	2.1	1.3		**diHCer**	2.1	5.0		**diHCer**	3.0	7.4
C24	**Cer**	1.5	2.5	**C24**	**Cer**	1.3	3.7	**C24**	**Cer**	2.1	5.2
	diHCer	1.9	1.9		**diHCer**	1.8	4.1		**diHCer**	1.6	2.7
C26	**Cer**	2.0	3.0	**C26**	**Cer**[e]	-	-	**C26**	**Cer**	0.9	1.7
	diHCer[e]	-	-		**diHCer**[e]	-	-		**diHCer**[e]	-	-

[a] Abbreviations: FC, fold change; 5h, 5h staurosporine-treated cells; 16h, 16h staurosporine-treated cells; C, control cells. [b] *m/z*'s corresponding to $[M-H]^-$. [c] *m/z*'s and the corresponding RT for each species can be found in the supplemental experimental procedure within lipid identification section. [d] FC was determined as [Abundance 16h or 5 h] / [Abundance C] for each lipid. Abundance is the total ion count for a given ion. Each ion corresponds to a mass-to-charge ratio (*m/z*), which is used to assign the lipid species. [e] Not detected.

SUPLEMENTAL EXPERIMENTAL PROCECURES

Cell lines and chemicals. hTERT RPE-1 (human retinal pigmented epithelium), HCT-116 (human colorectal carcinoma), HeLa S3 (human cervical carcinoma), and CCD-112CoN (human colon) were purchased from the American Type Culture Collection (Manassas, VA, USA). MCF-7 (human breast adenocarcinoma) cell line was kindly provided by Drs. Javier Blanco and Adolfo Quiñones Lombraña (Department of Pharmaceutical Sciences, University at Buffalo, Buffalo, NY, USA). Culture media (DMEM, EMEM, and DMEM/F-12 50/50), fetal bovine serum (FBS), penicillin/streptomycin mixture, and trypsin were bought from Corning (Manassas, VA, USA). Dimethylsulfoxide (DMSO), 3-(4,5-dimethylthiazol-2-yl)-2,5-diphenyltetrazolium bromide (MTT), α-tubulin antibody were purchased from Sigma-Aldrich, USA. PARP antibody was purchased from Cell Signaling. Staurosporine and doxorubicin were bought from Enzo and Tocris, and lipid standards from Avantipolar Lipids. LC-MS columns were obtained from Phenomenex. All other reagents were acquired from Sigma Aldrich and solvents were LC-MS grade.

Cell culture and treatments. HCT-116, HeLa S3 and MCF-7 were grown in DMEM and CCD-112 cells in EMEM. RPE-1 cell line was grown in DMEM/F-12 50/50 containing 0.3% (w/v) sodium bicarbonate. All cell culture media were supplemented with 10% (v/v) FBS, 100 U/mL penicillin, and 100 mg/mL streptomycin. Cell lines were maintained using standard incubation conditions at 37 °C and 5% CO_2. Cells were treated at 70-80% confluency. Twenty-four hours after seeding, cells were exposed to different times and concentrations of staurosporine, doxorubicin, C16-ceramide or -dihydroceramide at 37 °C.

Immunofluorescence and image acquisition. After 24 hours of seeding, cells were treated with 0.3 μM staurosporine. After treatment, the staining was carried out using the Apoptosis/Necrosis Detection Kit (ab176749, Abcam, Cambrigde, UK) following manufacturer's instructions. Images were acquired on a Leica DMI6000B inverted microscope using LAS AF software (Leica AF6000 Modular System, Leica Microsystems CMS GmbH, Germany).

LC-MS Method Data Analysis. The flow rate was 0.1 mL/min for the first 5 min followed by a change to 0.5 mL/min for the remainder of the gradient. A DualJSI fitted electrospray ionization (ESI) source was used for MS analysis with a capillary voltage of 3500 V and fragmentor voltage of 175 V. Drying gas temperature was 350 °C with a flow rate of 12 L/min. Data was collected using an *m/z* range of 50-1700 in extended dynamic mode. Tandem mass spectrometry data were collected using the following collision energies: 15, 35, 55, 75, 95 eV for each *m/z*.

For untargeted lipidomics, raw data obtained was imported into MassHunter Profinder (version B.06.00, Agilent Technologies) for peak alignment. For each profiling experiment, five biological replicates for the three conditions (control, 5h, and 16 h) were used. Data from Profinder was imported into Agilent Mass Profiler Professional (MPP, version B12.6.1) for statistical analysis where species were filtered based on frequency (60%). We conducted ANOVA to determine statistically significant species and eliminated all features with $p > 0.05$. Next, species were compared in a pairwise manner using three independent profiling experiments and we focused on the species that changed at least three fold across three independent profiling experiments. The resulting compounds were then matched to METLIN database to identify a candidate molecule based on accurate mass (Tautenhahn et al., 2012; Zhu et al., 2013). Known lipid standards (or lipids belonging to same lipid families) were purchased for the candidate lipids. MS/MS fragmentation patterns of the species of interest and known candidate lipids were compared. While fragmentation patterns were investigated, searches based on MS/MS fragments provided in METLIN were used complementary to the fragmentation pattern of known standards. For targeted analysis, the corresponding *m/z*'s for each ion were extracted in Agilent MassHunter Qualitative Analysis (version B.06.00). Peak areas for each ion were manually integrated and average abundances were calculated for each condition. Fold changes were subsequently calculated.

Droplet digital PCR (ddPCR). Quantification was performed with probe-based assays using pre-designed Integrated DNA Technologies (IDT, Coralville, IA, USA) Primers and ZEN double-quenched probes. Water-in-oil emulsion droplets were generated using an Automated Droplet Generator (Bio-Rad) and transferred to 96-well plates, which were heat-sealed using foil sheets. Target genes and the reference gene, *HPRT1* (hypoxanthine phosphoribosyltransferase 1) were amplified in parallel by thermal cycling the droplet emulsions as follows: 95 °C for 10 min (Taq DNA polymerase activation), 40 cycles of 94 °C for 30 s (denaturation), 56 °C for 60 s (annealing and extension) with a final 10 min inactivation step at 98 °C. The fluorescence of each thermally cycled droplet was measured using the QX200 droplet reader (Bio-Rad). Data was analyzed using the QuantaSoft software (Bio-Rad) after threshold setting on fluorescence of negative controls. Sequences of primers: *CERS1* sense 5-GCC TTC CAC AAC CTC CTG-3, antisense 5-AAC TGG GTA ACA AGC AGA GTC-3; *CERS2* sense 5-CAC TGC GTT CAT

CTT CTA CCA-3, antisense 5-GCT CTA TCC TGC CTT CTT TGG-3; *CERS3* sense 5-ACA TCA AAG CCA AGT CTA AAT AAC AG-3, antisense 5-GGC TAT ATG ACT TAT GGG AGG TT-3; *CERS4* sense 5-ACA TCA GAA GCC CGT TGA AG-3, antisense 5-CTC TTC CTC ATC TTC TCC TTT GTC-3; *CERS5* sense 5-CCG ATT ATC TCC CAA CTC TCA A-3, antisense 5-GCC AAT TAT GCC AAG TAT CAG C-3; *CERS6* sense 5-TGA CTC CGT AGG TAA ATA CAT AAA GG-3, antisense 5-CAA TCA GGA GAA GCC AAG CA-3; *HPRT1* sense 5-TTG TTG TAG GAT ATG CCC TTG A-3, antisense 5-GCG ATG TCA ATA GGA CTC CAG-3.

MTT Assay. After treatment, the plates were centrifuged, the medium was removed and 200 μL of media with 9% MTT (5 mg/mL in PBS) were added to each well. The plates were subsequently incubated for 3 h at 37 °C. After incubation, 150 μL of media were removed from each well and 90 μL of DMSO were added to each well. Treatments were carried out at a minimum of triplicates. The absorbance was measured using an automatic plate reader (Spectra MR™, Dynex technologies, Inc., Chantilly, VA, USA) at 550 nm. Cell viability was calculated as percentages relative to control cells.

Western blot analysis. Cells and media were collected in falcon tubes and centrifuged. The supernatant was discarded and cells were washed with PBS, and centrifuged. Cells were lysed with M-PER reagent (Thermo Scientific, Rockford, IL, USA) containing a protease inhibitor cocktail (Roche Diagnostics Indianapolis, IN, USA); debris was then removed by centrifugation and supernatant used for measuring protein concentration by Bradford assay (Thermo Scientific, Rockford, IL, USA). Equivalent amounts of protein were separated on 10% SDS-PAGE and transferred onto a nitrocellulose membrane (Bio-Rad Laboratories, Germany). Membranes were blocked with TBS-Tween [10 mM Tris-base, 100 mM NaCl, 0.1% Tween 20 (pH 7.5)] containing 5% nonfat dry milk, then washed with TBS-Tween and exposed to anti-PARP (PARP Rabbit Ab, Cell Signaling Technology, Danvers, MA, USA). After primary incubation, membranes were washed with TBS-Tween followed by incubation with anti-rabbit secondary antibody. Then, membranes were washed with TBS-Tween, and developed using the SuperSignal West Pico kit (Thermo Scientific, Rockford, IL, USA). Blots were stripped using stripping buffer [6.3 mmol/LTris-base, 0.2% SDS, 0.8 % (v/v) β-mercaptoethanol (pH 6.8)] and re-blotted for anti-tubulin in order to confirm equal protein loading.

Normalization and the matrix effect. Normalization across different samples was carried out based on protein concentration and the use of internal standards (Oleic acid-^{13}C18 and C17-ceramide). Ionization efficiencies based on total ion counts of the standards were investigated and corrected when necessary.

Quantification of ceramides by LC-MS. A dilution experiment was performed with a non-endogenous ceramide to quantify ceramides in HCT-116 and CCD-112 cells. Prior to extraction, samples were spiked with C17-ceramide as an internal standard. After extraction, serial dilutions of the samples were performed. These samples were analyzed using LC-MS QTOF in negative ESI mode. The data acquisition conditions were similar to that of profiling experiments. A calibration curve was obtained based on the ion counts and different concentrations of C17-ceramide in HCT-116 and CCD-112 cells separately. In order to use C17-ceramide as a standard to calculate the concentrations of endogenous ceramides, equal concentrations of C14-, C17-, C16-, C22- and C24-ceramide were prepared, injected into LC-MS QTOF and ion abundances were calculated. Based on this, response factors that account for differences in ionization efficiency were determined for C14-, C16-, C22- and C24- ceramides. Subsequently, C14-, C16-, C22- and C24-ceramide were quantified.

Media extraction. The growth media of staurosporine-treated and untreated HCT-116 were collected from which lipids were extracted. Briefly, a mixture of media:MeOH:$CHCl_3$ (1:1:2) was vortexed and allowed to settle (the procedure was repeated three times per sample). The sample was then centrifuged and the organic layer recovered from which 6 mL were taken and dried under vacuum. Finally, all the samples were resuspended in 200 μL of chloroform. The experiment was carried out in triplicate.

SUPPLEMENTAL LIPID ASSIGNMENTS

RT corresponds to retention time.

Standards.

C14-ceramide. Fragments generated in negative ionization mode. $[M-H]^-$ *m/z*: observed 508.4797; theoretical 508.4735. Observed fragments: 478.4704, 476.4534, 460.4570, 268.2360, 263.2456, 252.2416, 237.2315, 226.2232, 209.1996.

Fragments generated in positive ionization mode. $[M+H-H_2O]^+$ *m/z*: observed 492.4790; theoretical 492.4775. Observed fragments: 474.4668, 462.4668, 282.2791, 264.2689, 228.2319.

C14-dihydroceramide. Fragments generated in negative ionization mode. $[M-H]^-$ *m/z*: observed 510.4982; theoretical 510.4892. Observed fragments: 478.4734, 462.4790, 268.2393, 265.2601, 252.2445, 239.2481, 226.2295, 209.2024.

Fragments generated in positive ionization mode. $[M+H-H_2O]^+$ *m/z*: observed 494.4936; theoretical 494.4932. Observed fragments: 476.4817, 464.4785, 284.2946, 266.2833, 228.2327.

C22-ceramide. Fragments generated in negative ionization mode. $[M-H]^-$ *m/z*: observed 620.6047; theoretical 620.5987. Observed fragments: 590.5953, 588.5782, 572.5801, 380.3618, 364.3666, 338.3483, 321.3252, 263.2442, 237.2310.

Fragments generated in positive ionization mode. $[M+H-H_2O]^+$ *m/z*: observed 604.6036; theoretical 604.6027. Observed fragments: 586.5912, 574.5915, 340.3574, 282.2792, 264.2693.

C16-glucosylceramide. Fragments generated in negative ionization mode. $[M-H]^-$ *m/z*: observed 698.5570; theoretical 698.5576. Observed fragments: 536.5096, 280.2760, 263.2442, 255.2494, 237.2379, 179.0699.

Fragments generated in positive ionization mode. $[M+H-H_2O]^+$ *m/z*: observed 682.5622; theoretical 682.5616. Observed fragments: 664.5094, 520.5079, 502.4980, 282.2783, 264.2685, 256.2636, 145.0501, 121.0999, 95.0855.

IDENTIFICATION OF SPECIES FROM GLOBAL UNTARGETED PROFILING

Identification of *m/z*: 360.3093 (C18 FA derivative). RT 47.4. MS/MS fragments obtained were searched in METLIN. $[M+H+H_2O]^+$ m/z: observed 360.3093; theoretical 360.3108.Observed fragments: 342.3014, 284.2903, 267.2781, 266.2920, 76.0398.

Identification of *m/z*: 398.3278 (C16:1 acylcarnitine). RT 40.3. MS/MS fragments obtained were searched in METLIN. $[M]^+$ m/z : observed 492.4778; theoretical 492.4775. Observed fragments: 339.2516, 255.2351, 237.2206, 144.1036, 85.0332, 60.0848.

Identification of *m/z*: 492.4772 (C14-ceramide). RT 56.6. Fragmentation pattern was compared with ceramide standards. $[M+H-H_2O]^+$ *m/z*: observed 492.4778; theoretical 492.4775. Observed fragments: 474.4666, 462.4638, 282.2787, 264.2683, 228.2313.

Identification of *m/z*: 510.4841 (C14-dihydroceramide). RT 61.5. Fragmentation pattern was compared with dihydroceramide standard. $[M-H]^-$ *m/z*: observed 510.4810; theoretical 510.4892. Observed fragments: 478.4758, 462.4535, 268.2292, 252.2382, 239.2356, 226.2160, 209.1900.

Identification of *m/z:* 536.5007 (C16-ceramide). RT 62.7. Fragmentation pattern was compared with ceramide standards. $[M-H]^-$ *m/z*: observed 536.5042; theoretical 536.5048. Observed fragments: 506.4955, 504.4794, 488.4835, 280.2646, 237.2227.

Identification of *m/z:* 538.5163 (C16-dihydroceramide). RT 63.2. Fragmentation pattern was compared with dihydroceramide standard. $[M-H]^-$ *m/z*: observed 538.5188; theoretical 538.5205. Observed fragments: 506.4920, 490.4976, 296.2584, 280.2637, 265.2537, 254.2487, 239.2375, 237.2213.

Identification of *m/z:* 570.4603 (C16:1-ceramide). RT 61.2. Fragmentation pattern was compared with ceramide standards. $[M-Cl]^-$ *m/z*: observed 570.4691; theoretical 570.4658. Observed fragments: 237.2270, 235.2088.

Identification of *m/z:* 624.6283 (C22-dihydroceramide). RT 61.2. Fragmentation pattern was compared with dihydroceramide standard. $[M+H]^+$ *m/z*: observed 624.6281; theoretical 624.6289. Observed fragments: 606.6179, 588.6074, 340.3556, 302.3051, 284.2955, 266.2855.

Identification of *m/z:* 630.6178 (C24:1-ceramide). RT 61.7. Fragmentation pattern was compared with ceramide standards. $[M+H-H_2O]^+$ *m/z*: observed 630.6194; theoretical 630.6184. Observed fragments: 612.6081, 600.6074, 366.3728, 282.2787, 264.2687.

Identification of *m/z:* 648.6231 (C24:1-didhydroceramide). RT 68.2. Fragmentation pattern was compared with dihydroceramide standard. $[M-H]^-$ *m/z*: observed 648.6250; theoretical 648.6300. Observed fragments: 616.5997, 600.6116, 406.3619, 390.3762, 364.3541, 347.3308, 265.2378, 239.2403. The compound was identified as Cer(18:0/24:1).

Identification of *m/z:* 658.6477 (C26:1-ceramide). RT 62.6. Fragmentation pattern was compared with ceramide standards. $[M+H-H_2O]^+$ *m/z*: observed 658.6497; theoretical 658.6497. Observed fragments: 640.6387, 628.6442, 340.3574, 394.4079, 282.2813, 264.2708. The compound was identified as Cer(18:1/26:1).

Identification of *m/z:* 677.5607 (C14-dihydrosphingomyelin). RT 54.9. Fragmentation pattern was compared with dihydroceramide standard and MS/MS fragments provided in METLIN metabolite database. $[M]^+$ *m/z*: observed 677.5609; theoretical 677.5592. Observed fragments: 659.5458, 600.4703, 494.4903, 252.2352, 266.2886, 228.2402, 184.0779, 166.0669, 125.0038, 86.1004.

Identification of *m/z:* 810.6744 (C24:1-hexosyldihydroceramide). RT 66.4. Fragmentation pattern was compared with hexose- and dihydro-ceramide standard. $[M-H]^-$ *m/z*: observed 810.6802; theoretical 810.6828. Observed fragments: 752.5916, 648.6291, 616.6018, 600.6096, 406.3673, 390.3807, 364.3539, 347.3375, 265.2550, 239.2319, 179.0616, 161.0478.

Identification of *m/z:* 815.7018 (C24:1-dihydrosphingomyelin). RT 60.8. Fragmentation pattern was compared with dihydroceramide standard and MS/MS fragments provided in METLIN metabolite database. $[M]^+$ *m/z*: observed 815.7020; theoretical 815.7001. Observed fragments: 797.6849, 738.6064, 632.6289, 614.6190, 284.2913, 266.2842, 184.0740, 166.0628, 125.0000, 86.0971.

Identification of *m/z:* 817.7147 (C24-dihydrosphingomyelin). RT 61.4. Fragmentation pattern was compared with dihydroceramide standard and MS/MS fragments provided in METLIN metabolite database. $[M]^+$ *m/z*: observed 817.7120; theoretical 817.7157. Observed fragments: 799.7124, 740.6381, 676.6314, 634.6362, 368.3945, 266.2840, 184.0730, 166.0648, 125.0005, 86.0990.

Identification of *m/z:* 841.7160 (C26:1-sphingomyelin). **RT 61.2.** Fragmentation pattern was compared with ceramide standards and MS/MS fragments provided in METLIN metabolite database. $[M]^+$ *m/z*: observed 841.7130; theoretical 841.7157. Observed fragments: 823.7032, 764.6304, 658.6466, 640.6365, 418.3986, 264.2655, 184.0710, 166.0573, 124.9972, 86.0947.

IDENTIFICATION OF SPECIES FROM TARGETED ANALYSIS

RT corresponds to retention times.

Ceramides

C14-ceramide. RT 60.9. The compound was assigned based on the fragmentation pattern found by the ceramide standards. $[M-H]^-$ *m/z*: observed 508.4698; theoretical 508.4735. Observed fragments: 476.4566, 460.4527, 252.2295, 237.2184, 226.2047, 209.1992.

C16-ceramide. RT 62.7. The compound was assigned based on the fragmentation pattern found by the ceramide standards. $[M-H]^-$ *m/z*: observed 536.5044; theoretical 536.5048. Observed fragments: 506.4897, 504.4753, 488.4793, 280.2627, 237.2202.

C18-ceramide. RT 64.3. The compound was assigned based on the fragmentation pattern found by the ceramide standards. $[M-H]^-$ *m/z*: observed 564.5319; theoretical 564.5361. Observed fragments: 534.5205, 532.5055, 516.5113, 308.2927, 282.2789, 265.2523, 237.2217.

C20-ceramide. RT 65.7. The compound was assigned based on the fragmentation pattern found by the ceramide standards. $[M-H]^-$ *m/z*: observed 592.5640; theoretical 592.5674. Observed fragments: 562.5579, 560.5370, 544.5417, 336.3249, 310.3076, 293.2841, 237.2233.

C22-ceramide. RT 66.2. The compound was assigned based on the fragmentation pattern found by the ceramide standards. $[M-H]^-$ *m/z*: observed 620.5944; theoretical 620.5987. Observed fragments: 590.5822, 588.5648, 572.5729, 364.3553, 338.3398, 321.3110, 237.2211.

C24-ceramide. RT 67.3. The compound was assigned based on the fragmentation pattern found by the ceramide standards. [M-H]- *m/z*: observed 648.6245; theoretical 648.6300. Observed fragments: 618.6138, 616.5990, 600.6056, 392.3960, 237.2203.

C26-ceramide. RT 69.1. The compound was assigned based on the fragmentation pattern found by the ceramide standards. $[M-H]^-$ *m/z*: observed 676.6655; theoretical 676.6613. Observed fragments: 646.6543, 644.6414, 628.6500, 420.4269, 394.4041, 377.3809, 237.2313.

Dihydroceramides

C14-dihydroceramide. RT 61.5. The compound was assigned based on the fragmentation pattern found by the dihydroceramide standard. $[M-H]^-$ *m/z*: observed 510.4918; theoretical 510.4892. Observed fragments: 478.4624, 462.4692, 252.2374, 239.2470, 209.1973.

C16-dihydroceramide. RT 63.2. The compound was assigned based on the fragmentation pattern found by the dihydroceramide standard. $[M-H]^-$ *m/z*: observed 538.5211; theoretical 538.5205. Observed fragments: 506.4965, 490.5012, 280.2676, 239.2412, 237.2254.

C18-dihydroceramide. RT 64.7. The compound was assigned based on the fragmentation pattern found by the dihydroceramide standard. $[M-H]^-$ *m/z*: observed 566.5568; theoretical 566.5518. Observed fragments: 534.5300, 518.5332, 308.3019, 265.2575, 239.2459.

C20-dihydroceramide. RT 66.1. The compound was assigned based on the fragmentation pattern found by the dihydroceramide standard. $[M-H]^-$ *m/z*: observed 594.5879; theoretical 594.5831. Observed fragments: 564.5659, 562.5659, 336.3357, 293.2909, 239.2459.

C22-dihydroceramide. RT 67.3. The compound was assigned based on the fragmentation pattern found by the dihydroceramide standard. $[M-H]^-$ m/z: observed 622.6212; theoretical 622.6144. Observed fragments: 590.5906, 574.5965, 364.3657, 321.3210, 239.2448.

C24-dihydroceramide. RT 68.5. The compound was assigned based on the fragmentation pattern found by the dihydroceramide standard. $[M-H]^-$ *m/z*: observed 650.6480; theoretical 650.6457. Observed fragments: 618.6222, 602.6281, 392.3967, 349.3528, 239.2403.

Sphingomyelins

C14-sphingomyelin. RT 53.8. The compound was assigned based on the fragmentation pattern found by ceramide standards and MS/MS fragments provided in METLIN metabolite database. $[M]^+$ *m/z*: observed 675.5419; theoretical 675.5436. Observed fragments: 657.5286, 598.4701, 474.4646, 264.2683, 252.2326, 184.0725, 166.0622, 124.9995, 86.0967.

C16-sphingomyelin. RT 55.3. The compound was assigned based on the fragmentation pattern found by ceramide standards and MS/MS fragments provided in METLIN metabolite database. $[M]^+$ *m/z*: observed 703.5722; theoretical 703.5749. Observed fragments: 685.5635, 626.4875, 502.4933, 280.2684, 264.2688, 184.0740, 166.0635, 125.0005, 86.0981.

C18-sphingomyelin. RT 56.8. The compound was assigned based on the fragmentation pattern found by ceramide standards and MS/MS fragments provided in METLIN metabolite database. $[M]^+$ *m/z*: observed 731.6091; theoretical 731.6062. Observed fragments: 713.6046, 530.5130, 264.2700, 184.0736, 166.0620, 124.9999, 86.0973.

C22-sphingomyelin. RT 59.5. The compound was assigned based on the fragmentation pattern found by ceramide standards and MS/MS fragments provided in METLIN metabolite database. $[M]^+$ *m/z*: observed 787.6664; theoretical 787.6688. Observed fragments: 769.6508, 603.5366, 364.3449, 264.2676, 184.0739, 166.0603, 125.0003, 86.0980.

C24-sphingomyelin. RT 61.1. The compound was assigned based on the fragmentation pattern found by ceramide standards and MS/MS fragments provided in METLIN metabolite database. $[M]^+$ *m/z*: observed 815.7054; theoretical 815.7001. Observed fragments: 797.6888, 738.6164, 674.6172, 632.6277, 614.6227, 392.3890, 264.2705, 184.0743, 166.0620, 125.0004, 86.0974.

C24-sphingomyelin. RT 65.1. The compound was assigned based on the fragmentation pattern found by ceramide standards and MS/MS fragments provided in METLIN metabolite database. $[M]^+$ *m/z*: observed 843.7285; theoretical 843.7314. Observed fragments: 825.6981, 642.6367, 264.2674, 184.0695, 166.0595, 124.9967, 86.0944.

Dihydrosphingomyelins

C14-dihydrosphingomyelin. RT 54.9. The compound was assigned based on the fragmentation pattern found by dihydroceramide standard and MS/MS fragments provided in METLIN metabolite database. $[M]^+$ *m/z*: observed 677.5522; theoretical 677.5592. Observed fragments: 659.4223, 600.4842, 494.4885, 266.2783, 252.2352, 184.0718, 166.0602, 124.9968, 86.0954.

C16-dihydrosphingomyelin. RT 56.5. The compound was assigned based on the fragmentation pattern found by dihydroceramide standard and MS/MS fragments provided in METLIN metabolite database. $[M]^+$ *m/z*: observed 705.5893; theoretical 705.5905. Observed fragments: 687.5880, 628.5065, 522.5313, 504.5008, 280.2644, 266.2814, 184.0733, 166.0619, 124.9999, 86.0973.

C24-dihydrosphingomyelin. RT 61.6. The compound was assigned based on the fragmentation pattern found by dihydroceramide standards and MS/MS fragments provided in METLIN metabolite database. $[M]^+$ *m/z*: observed 817.7120; theoretical 817.7157. Observed fragments: 799.7124, 740.6381, 676.6314, 634.6362, 368.3945, 266.2840, 184.0730, 166.0648, 125.0005, 86.0990.

SUPPLEMENTAL REFERENCES

Tautenhahn, R., Cho, K., Uritboonthai, W., Zhu, Z., Patti, G.J., and Siuzdak, G. (2012). An accelerated workflow for untargeted metabolomics using the METLIN database. Nat Biotechnol *30*, 826-828.

Zhu, Z.J., Schultz, A.W., Wang, J., Johnson, C.H., Yannone, S.M., Patti, G.J., and Siuzdak, G. (2013). Liquid chromatography quadrupole time-of-flight mass spectrometry characterization of metabolites guided by the METLIN database. Nat Protoc *8*, 451-460.